




# A LLZO Fibers/ PPO polymeric matrix solid electrolyte for high voltage solid-state lithium batteries

Liang Zhong<sup>1</sup> · Jie Li<sup>1</sup> · Zhi-xiong Chen<sup>2</sup> · Li-ping Zhou<sup>3</sup> · Hai-xia Liu<sup>1</sup> · Xiang-qian Shen<sup>1</sup> · Mao-xiang Jing<sup>1</sup> 

Received: 27 April 2024 / Accepted: 9 August 2024 / Published online: 29 August 2024  
© The Author(s), under exclusive licence to Springer-Verlag GmbH Germany, part of Springer Nature 2024

## Abstract

Low ionic conductivity, narrow electrochemical window and poor mechanical property are the core problems that polymer solid electrolyte is difficult for practical application. Choosing suitable polymer and regulating the ion transport path through inorganic fillers is an important method to solve the above problems. Herein, a polymeric matrix composite solid electrolyte(CSE) was achieved by combining electrospun  $\text{Li}_7\text{La}_3\text{Zr}_2\text{O}_{12}$  (LLZO) fibers and highly viscoelastic polypropylene oxide(PPO). The PPO matrix provides the CSE with good mechanical property to 56.75 MPa. While the addition of fibrous LLZO improves the ion transport channels of the CSE, which boosts the ionic conductivity, electrochemical window and ion transport number up to  $4.59 \times 10^{-4} \text{ S cm}^{-1}$  at room temperature, 5.4 V and 0.74, respectively, when the content of LLZO fiber is 7.5 wt% of PPO polymer. The prepared PPO-LLZO fibers electrolyte can be used in high-voltage solid-state lithium battery and shows good rate and cycle performances. This composite solid electrolyte film and its simplified preparation conditions is beneficial for practical applications in solid-state batteries.

**Keywords** Composite solid electrolyte · LLZO fiber · Polypropylene oxide · Ion transport path

## 1 Introduction

Solid-state lithium batteries with higher safety and greater energy density have attracted extensive attention from scientists [1, 2]. Solid electrolyte, as an important component of solid-state batteries, determines the safety and electrochemical performances of solid-state batteries [3, 4]. However, it also faces many critical problems, such as low ionic conductivity, narrow electrochemical window, poor mechanical properties and high interfacial impedance, which hinders the improvement of solid-state battery's performances and its wide application [5, 6].

Compared with ceramic electrolyte or pure polymer electrolyte, the organic/inorganic composite solid electrolytes (CSEs) combining suitable rigid inorganic fillers and flexible polymer solid electrolytes not only can improve the problems of low ionic conductivity and high interfacial impedance, but also enhance the thermal and mechanical properties of polymer electrolyte, which are becoming the most promising technology direction for industrial application (7, 8, 9, 10). For instance,  $\text{Al}_2\text{O}_3$  combined with polyethylene oxide (PEO-AO) [11],  $\text{Li}_7\text{La}_3\text{Zr}_2\text{O}_{12}$ (LLZO) with PEO(PEO-LLZO) [12], LLZO with polyvinylidene fluoride (PVDF-LLZO) [13],  $\text{TiO}_2$  with propylene polycarbonate (PPC- $\text{TiO}_2$ ) [14, 15], etc. solid electrolytes were reported successively. Compared with pure polymer electrolytes, the thermal, mechanical and electrochemical properties of these CSEs have been enhanced. However, the enhancement of electrochemical properties is limited, because most polymers themselves have low ion conductivity and narrow potential window, and the added inorganic nanoparticles usually do not form continuous ion transport channels, so that they will not play a better role in ion transport. Cui and Hu et al. tried to add LLZO,  $\text{Li}_{0.34}\text{La}_{0.56}\text{TiO}_3$ (LLTO) and other nanowires or fibers to the traditional polymers [14, 16], they found that the ionic conductivity of the electrolyte

---

Liang Zhong and Jie Li contributed equally to this work.

✉ Mao-xiang Jing  
mxjing2004@ujs.edu.cn

<sup>1</sup> Institute for Advanced Materials, School of Materials Science and Engineering, Jiangsu University, Zhenjiang 212013, China

<sup>2</sup> Yangzhou Junhe Film Technology CO, Yangzhou 211400, China

<sup>3</sup> Anhui Yijiatong Battery Co., Ltd, Xuancheng 242000, China

was more improved compared with that of nanoparticles. This indicates that the quasi-one-dimensional fillers have more advantages over the nanoparticles in improving the ion transport path of the polymer electrolytes. However, due to the use of the traditional polymer, the mechanical, thermal and electrochemical properties of the composite electrolyte still need to be further improved.

In recent years, some new polymers, inorganic fillers and organic / inorganic composite methods have been explored [17–19]. Xu et al. [9] found that polypropylene oxide (PPO) polymer has the advantages of high ionic conductivity at room temperature, good viscoelasticity, and high heat-resistance temperature, which is more suitable for solid electrolyte compared with the traditional polymers such as PEO [20, 21], PPC [22], PVDF [23, 24]. They prepared 40  $\mu\text{m}$ -thick PPO-ZrO<sub>2</sub> composite electrolyte with high ionic conductivity and good thermal and mechanical performances. On this basis, Li et al. also developed PPO-LLZO nanoparticle composite electrolyte [25]. The purpose of this work is to use high-filling content of LLZO particles to form continuous ion transport channels, but perhaps because of the serious agglomeration of LLZO nanoparticles, the actual performance has not increased significantly.

In our previous work [26] we prepared PPO/Al<sub>2</sub>O<sub>3</sub> fibers CSE, Al<sub>2</sub>O<sub>3</sub> fibers use the continuous interface to enhance the ion transport capacity. But Al<sub>2</sub>O<sub>3</sub> is a non-ionic conductor, so it does not have an effect on the ion transport itself. LLZO is an ionic conductor, and it is possible to obtain better electrochemical properties if replacing Al<sub>2</sub>O<sub>3</sub> fibers with LLZO fibers. [27]. Therefore, in this work, we first prepared

LLZO nanofibers by electrospinning method, and combined them with PPO to form a composite solid electrolyte film. Good viscoelastic PPO and porous skeleton provide high mechanical and thermal properties for the electrolyte, while LLZO fibers provide continuous ion transport channels based on their own ion conductivity and the interface. This organic/inorganic combination design helps to develop a practical solid electrolyte that integrates high mechanical, thermal and electrochemical properties, suitable for high-voltage solid-state batteries.

## 2 Experimental

The preparation of solid electrolyte in this study is mainly divided into two steps, including the preparation of LLZO nanofibers by electrostatic spinning method and the preparation of composite films by scratch coating method. LLZO fibers were obtained by a conventional electrostatic spinning method, and the preparation process is shown in Fig. 1. According to the stoichiometric ratio of LLZO, 0.9 g of Al(NO<sub>3</sub>)<sub>3</sub>·9H<sub>2</sub>O, 9.75 g of La(NO<sub>3</sub>)<sub>3</sub>·6H<sub>2</sub>O, 7.05 g of CH<sub>3</sub>COOLi, 8.59 g of Zr(NO<sub>3</sub>)<sub>4</sub>·5H<sub>2</sub>O, and were dissolved in 10 g of N, N-dimethylformamide (DMF) and 3.68 g of acetic acid was added to adjust the pH value of the solution in order to help the dissolution of metal salts. The solution was stirred in a magnetic stirrer for more than 10 h until all the materials were dissolved, and then it was recorded as solution (A). Then, 6 g of PVP was added to 30 g of DMF, and it was stirred until the polymer was completely

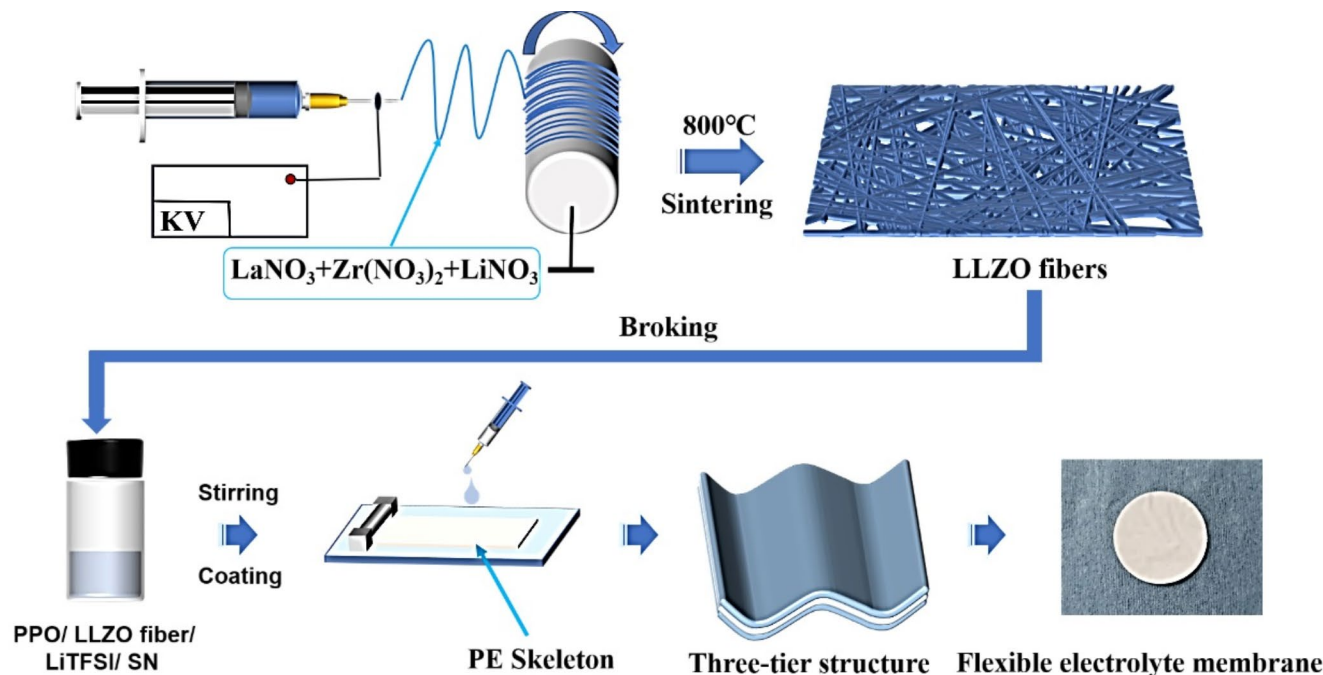


Fig. 1 Preparation process chart of LLZO fibers/PPO composite solid electrolyte

dissolved, it was recorded as solution (B) Solution B was placed in a 60 °C water bath stirrer and stirred. A burette was used to suck up the solution A and add it slowly to solution B, until two of them were mixed completely to form a homogeneous solution. The spinning liquid precursor was obtained. Next, the spinning precursor was electrospun into a composite fiber precursor at a feed rate of 0.2 ml h<sup>-1</sup>, a collection drum diameter of 100 mm, a winding speed of 200 r min<sup>-1</sup>, and a spinning voltage of 21 kV. Finally, the precursor fibers were calcined in air atmosphere at 800 °C for 2 h to obtain the desired LLZO fibers.

For the preparation step of electrolyte film, weighing LLZO fibers (masses of 2.5, 5, 7.5 and 10 wt% of the total PPO mass), 0.4 g of LiTFSI, and 0.1 g of LiBOB and dissolving them in 2.5 g of NMP solution, adding 2 g of PPO and 0.6 g of butanedinitrile to the solution. The homogeneous slurry was obtained after stirring for 12 h at room temperature. A certain amount of slurry was poured onto a polytetrafluoroethylene (PTFE) plate, and the first layer of slurry was scraped onto the PTFE plate with a scraper whose thickness was adjusted to 150 μm, and then a polyethylene(PE) film(9 μm) was overlaid on the first layer of slurry as a supporting skeleton, and after 5 min of standing, the thickness of the scraper was adjusted to 200 μm, and the second layer of slurry was scraped onto the PE film. The whole plate and electrolyte film were put into the 80°C blast drying oven for 12 h. The electrolyte film was separated from the PTFE plate, continue drying in vacuum drying oven at 100 °C for 12 h. Last, the film was transferred to the argon glove box, and cut into a 19 mm round piece for use.

The cathode preparation and all the characterization methods were described in the supporting file. And all the tests were implemented at room temperature (25°C).

### 3 Results and discussion

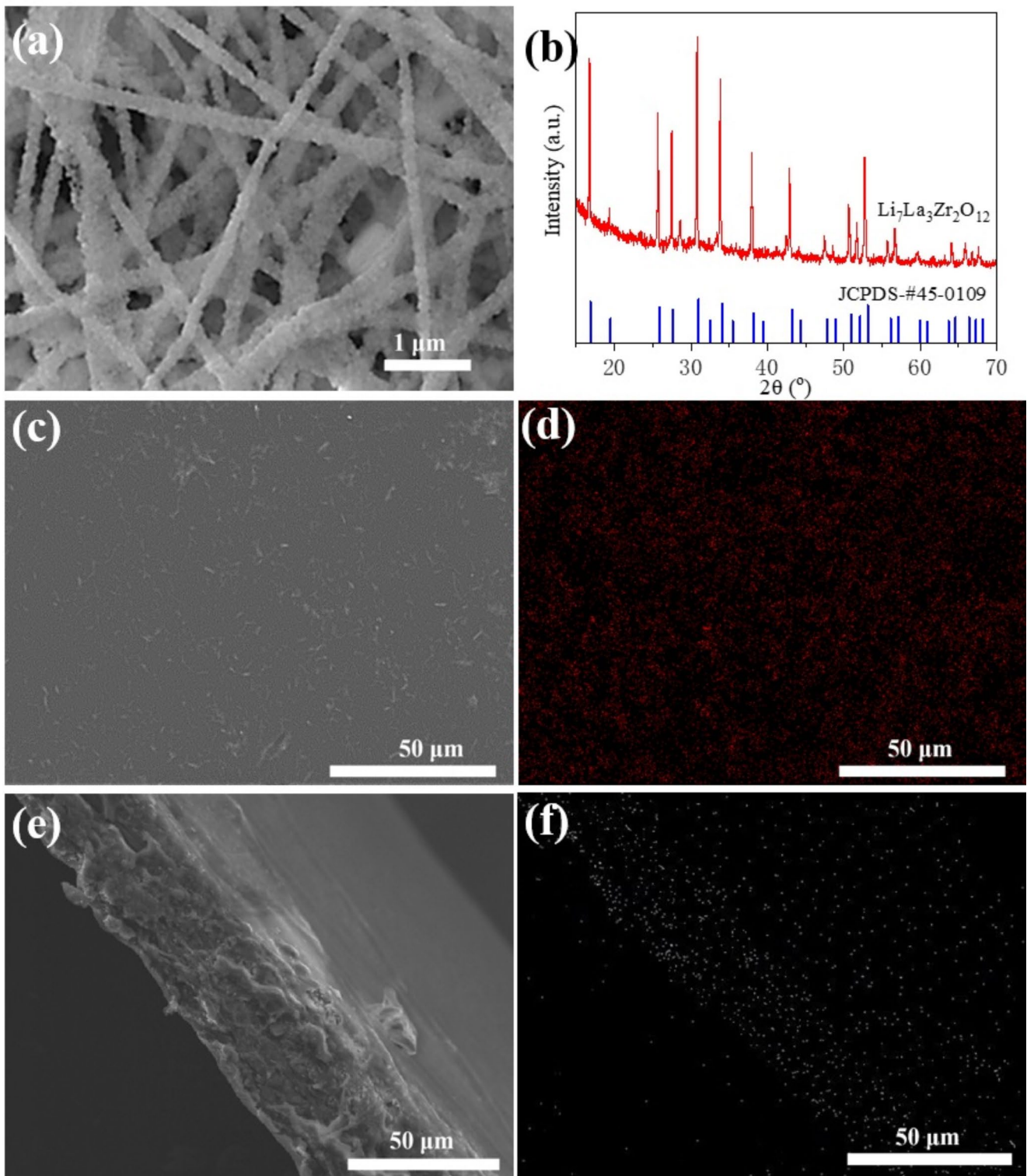
Figure 2(a, b) shows the SEM images and XRD spectra of the prepared LLZO fibers. It can be seen that the LLZO has obvious fiber morphology and the crystalline phase is pure LLZO. Figure 2(c) shows the surface SEM image of PPO-LLZO fiber CSE, the LLZO fibers are uniformly distributed on the electrolyte surface. This result can also be verified from the distribution mapping of Zr element in Fig. 2(d). From the figure, it can be seen that the mapping points are heavily and uniformly distributed in the PPO polymer matrix. Figure 2(e) shows the cross-section of the PPO-LLZO fiber CSE, and the thickness of the electrolyte is about 50 μm, while the distribution of Zr element in the cross-section of the electrolyte is still distributed uniformly as seen from the mapping diagram of Zr element in Fig. 2(f), which suggests that the LLZO fibers penetrate into and are

tightly wrapped by the PPO polymer matrix. This kind of light and thin composite electrolyte with compact structure facilitates the shuttle of lithium ions in the electrode/electrolyte and improves the ion transport performance [28].

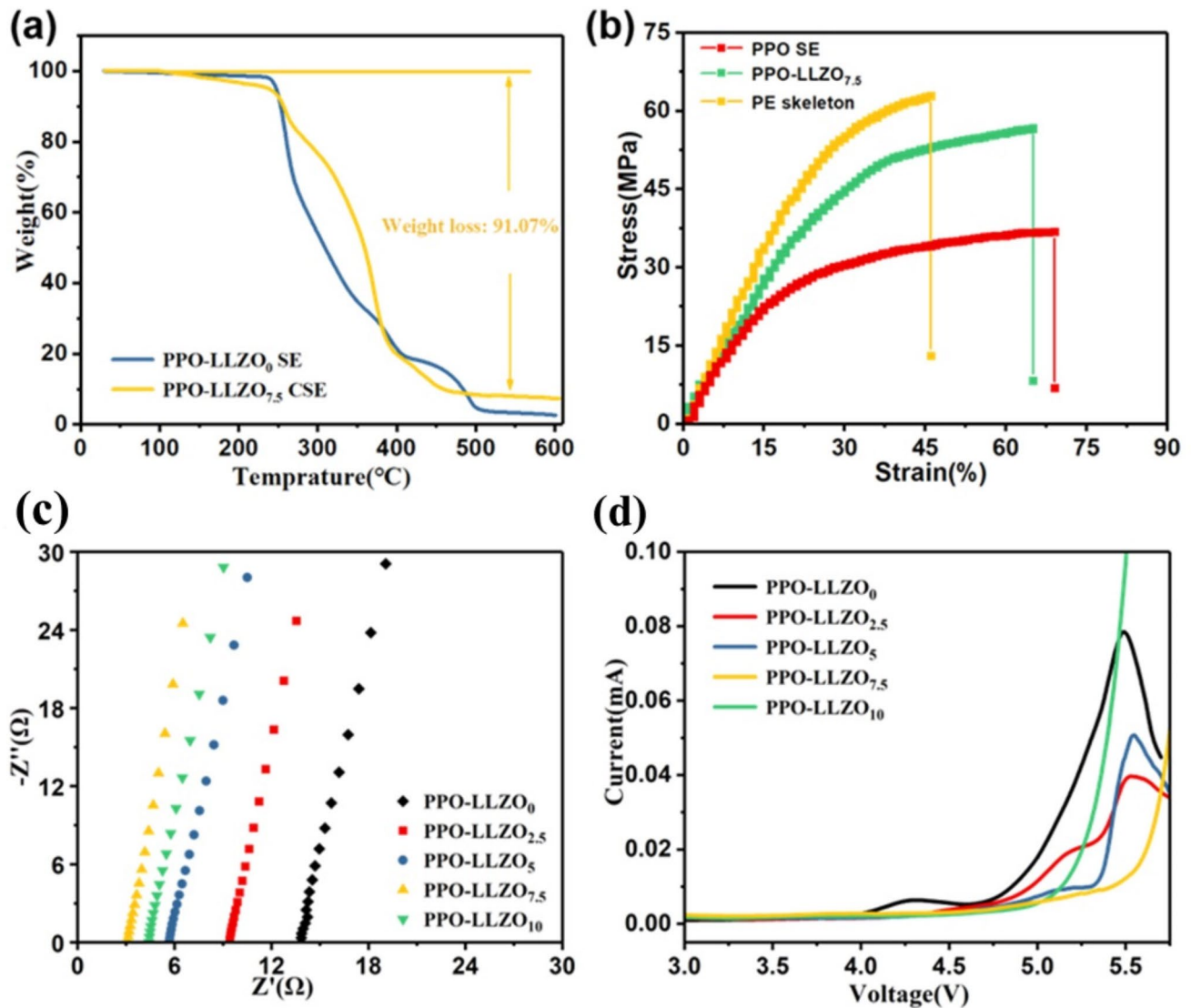
Figure S1 in the supporting file shows the FTIR spectra for PPO, PPO polymer electrolyte without LLZO fibers and PPO-LLZO composite electrolyte. From the enlarged infrared spectrum, it is obtained that the characteristic peaks at 1804 and 1778 cm<sup>-1</sup> are acids produced by the reaction of LiBOB [29]. In addition, the hydroxyl peak at 1194 cm<sup>-1</sup> can prove that it is present on the electrolyte and cannot come from water, due to the fact that the electrolyte film is in a dry state. The peaks of TFSI<sup>-</sup> in lithium salts appeared at 740, 1135, and 1333 cm<sup>-1</sup> and the peak intensity at 1133 cm<sup>-1</sup> increased due to the fact that the Lewis acid provided by the LLZO fibers interacts with TFSI<sup>-</sup> and promotes the dissociation of LiTFSI [30, 31]. The characteristic peaks at 990 and 1060 cm<sup>-1</sup> are due to the symmetric vibrations of the Si-O-Si bond caused by the polymerization reaction of PPO. Changes in these peaks indicate that the cross-linking reaction occurs in oligomeric PPO and forms long chains, and that the LLZO fibers do not chemically react with the polymer electrolyte [32].

Figure 3a shows the thermal analysis curve of PPO-LLZO fiber CSE. There is a slight weight loss of about 3% from room temperature to 250 °C, which is caused by the evaporation of solvent molecules adsorbed on the surface. PPO-LLZO<sub>0</sub> CSE begins to decompose from about 250 °C, while PPO-LLZO<sub>7.5</sub> CSE shows an initial decomposition at about 260 °C until a mass loss of about 91.04% at 460 °C, the residual weight is the LLZO fibers and lithium salts. This result suggests that PPO-LLZO CSE has good thermal stability. Figure 4b shows the stress-strain curves of PE skeleton, PPO polymer electrolyte without LLZO fibers and PPO-LLZO<sub>7.5</sub> CSE. The PPO polymer electrolyte without LLZO fibers has lower tensile strength of 36.27 MPa. After adding 7.5% LLZO fiber in the PPO matrix, the composite electrolyte shows better mechanical properties, and the tensile strength reaches 56.75 MPa, of course, such a high tensile strength is mainly due to the support of the PE skeleton, whose tensile strength is as high as 62.72 MPa, This high mechanical strength can avoid the short-circuit of the battery and inhibit the growth of lithium dendrites, thus improve the safety and stability of the battery [33, 34].

Figure 3c shows the electrochemical impedance spectra (EIS) curves for the ionic conductivity of composite electrolytes at room-temperature with different LLZO fiber contents. The ionic conductivity of the composite electrolyte gradually increases with the increase of LLZO fiber content, and the maximum ionic conductivity of CSE is up to 4.59 × 10<sup>-4</sup> S cm<sup>-1</sup> when the LLZO fiber content is 7.5 wt%. The high ionic conductivity is mainly due to the addition of



**Fig. 2** SEM image (a) and XRD pattern (b) of LLZO fibers, surface and cross-sectional SEM images (c, e) and corresponding element mapping of Zr



**Fig. 3** (a) TG curves of the PPO SE, and PPO-LLZO<sub>7.5</sub>, (b) Stress–strain curves of the PE skeleton, PPO SE, and PPO-LLZO<sub>7.5</sub>, (c) Impedance spectra of PPO-LLZO with different LLZO fiber content, (d) Electrochemical window of PPO-LLZO with different LLZO fiber content

LLZO fibers to the PPO polymer matrix, LLZO as fast ionic conductor can provide more free lithium ions from itself and Lewis acid-base reaction between LLZO with LiTFSI salt [35], meanwhile in comparison with the particles as fillers, one-dimensional linear materials are no longer point-to-point contacts, can provide continuous Li<sup>+</sup> transport channels [36, 37]. A slight increase in impedance can be observed when LLZO fiber content is up to 10 wt%, leading to a decrease in ionic conductivity, which may be due to the cross overlapping of fibers with excessive content, resulting in coarse surface and poor interface contact between electrode and electrolyte and hindering the ion migration. Figure 3d shows the electrochemical stability window curves of the PPO-LLZO CSE, which follows the same trend as that of the ionic conductivity, and the PPO polymer electrolyte

without LLZO fibers starts to show fluctuations at 4.0 V with very poor stability. The electrochemical window of CSE has a maximum value of 5.4 V when the LLZO fiber content is 7.5 wt%. Fig. S2 shows the steady-state polarization curve of the PPO-LLZO<sub>7.5</sub> CSE, and the inset shows the impedance spectra before and after polarization of the Li/PPO-LLZO<sub>7.5</sub>/Li cell. Calculation from ion transport number equation shows that the PPO-LLZO<sub>7.5</sub> CSE has an ion transport number up to 0.74. The ion transport numbers of CSEs with other LLZO fiber contents are also listed in Table S1 in the supporting information. From the results, it can be concluded that the introduction of LLZO fibers greatly improves the ion transport ability of PPO-based polymer electrolytes. These characteristic performances

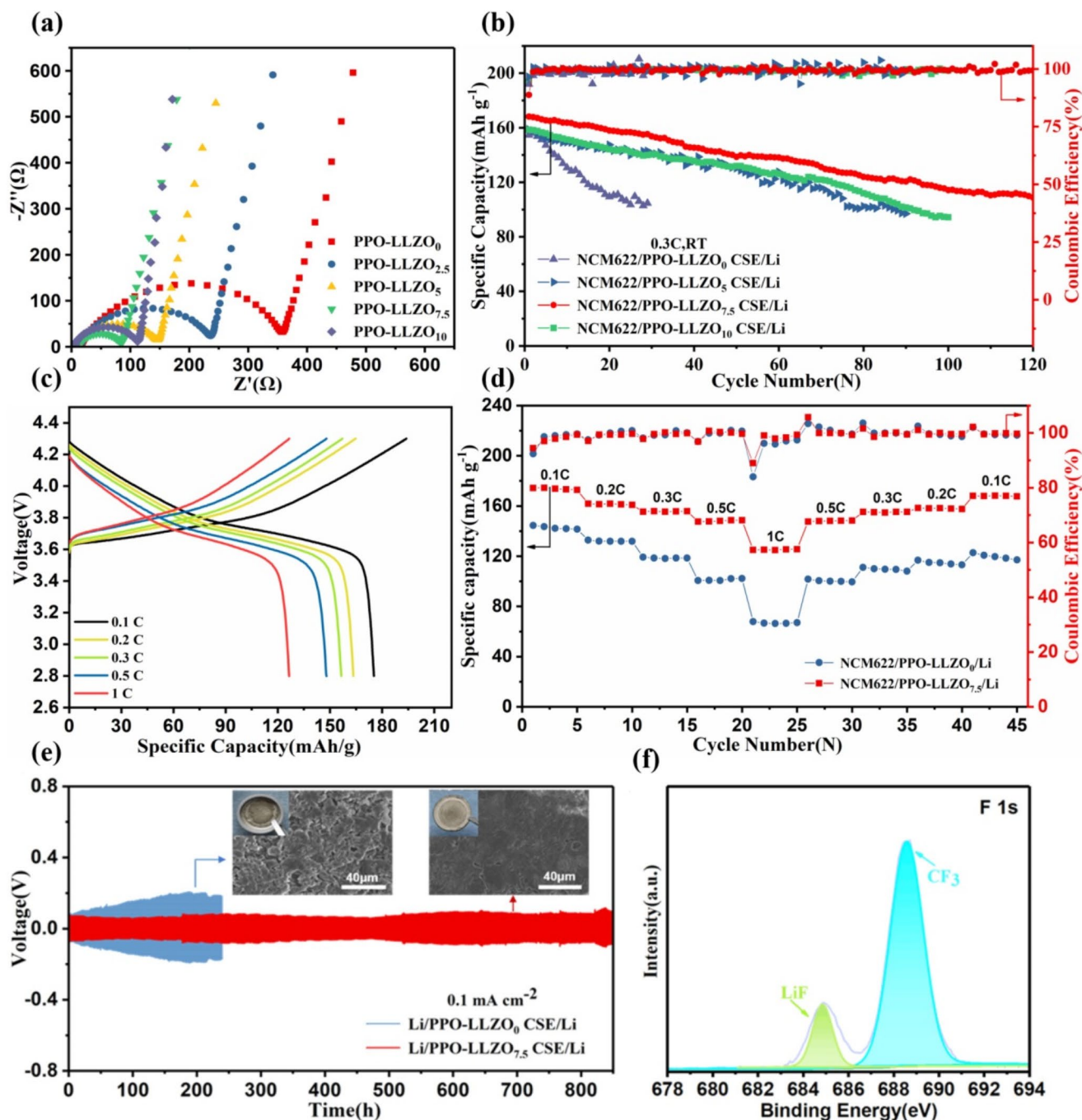


**Fig. 4** Performances of NCM622/ PPO-LLZO CSE/Li cells at room temperature, **(a)** EIS curves, **(b)** Cyclic performance, **(c)** Charge-discharge curves at different rates, **(d)** Rate performance, **(e)** Voltage-time

curves of Li plating/stripping cycle for Li/ CSE/Li cells, **(f)** XPS curves of F 1s on lithium sheet after cycle of the cell with PPO-LLZO<sub>7.5</sub> CSE

have obvious advantages over the relevant literatures (Table S2 in the supporting file) [9, 10, 12, 27].

The assembled NCM622/PPO-LLZO CSE/Li cells were further investigated for their electrochemical performances. The corresponding EIS curves are shown in Fig. 4(a). The cell without LLZO fibers has a maximum impedance up to 357  $\Omega$ , which also determines poor rate performance and

cycling performance. However, for cells with composite solid electrolytes containing LLZO fibers, the impedance decreases obviously with the increasing content of LLZO fibers, and the cell has the smallest impedance ( $\sim 80 \Omega$ ) at a content of 7.5 wt %, which corresponds to the highest ionic conductivity as described previously.

Figure 4b shows the cycling performance of the cells with different LLZO fiber contents at a current density of 0.3 C. It is clearly observed that the discharge specific capacity of the cell with the electrolyte without LLZO fiber decays rapidly after only several charging/discharging cycles. While the cell containing PPO-LLZO<sub>7.5</sub> CSE shows the best cycling performance with a first discharge capacity of 168.1 mAh g<sup>-1</sup> at a current density of 0.3 C and a capacity retention of 78% after 120 cycles, which further suggests that continuous Li<sup>+</sup> channels constructed by LLZO fibers improve the cycling performance of the cell [36, 37].

Rate performance tests were performed on cells containing CSE with 0% and 7.5% LLZO fiber contents (as shown in Fig. 3d). Obviously, the cell with 7.5 wt% LLZO CSE had better rate performance. The discharge specific capacities reached 174.4, 161.8, 155.5, 147.6 and 125.1 mA h g<sup>-1</sup> at 0.1, 0.2, 0.3, 0.5 and 1 C, respectively. When returning to 0.1 C again, the capacity is basically back to the initial state, representing good reversibility of the solid-state battery. In contrast, the discharge specific capacity of the cell without LLZO fibers decays to 67.9 mAh g<sup>-1</sup> at a current density of 1 C, which is not conducive to stable cycling at high rate.

Figure 4e shows the Li plating/stripping cycle profile of Li/ PPO-LLZO CSE /Li symmetric cell. Compared with the PPO polymer electrolyte without LLZO fibers, the cell containing PPO-LLZO<sub>7.5</sub> CSE can be stably cycled for about 850 h without significant change in overpotential, which indicates that the composite electrolyte film filled with LLZO fibers has a good stability to lithium metal. The inset image shows the SEM pictures of lithium sheets recycled from the cells containing PPO-LLZO<sub>0</sub> CSE and PPO-LLZO<sub>7.5</sub> CSE after cycling. The surface of lithium sheet corresponding to PPO polymer electrolyte without LLZO fibers becomes very rough, and many dead lithium produced from dendrites can be observed. In comparison, the lithium sheet corresponding to PPO-LLZO<sub>7.5</sub> CSE is smooth and looks metallic lustre. This difference is mainly attributed to the high mechanical strength of the composite electrolyte and the generation of a relatively stable SEI interface between the CSE and lithium metal, which inhibits the growth of lithium dendrites. Moreover, the LiF and CF<sub>3</sub> compositions in the SEI layer are also confirmed by the XPS analysis in Fig. 4d, which have been proved to be helpful to avoid the destruction of the interfacial layer by lithium dendrites [38–40].

## 4 Conclusions

In summary, a LLZO fiber/PPO composite solid electrolyte film was successfully prepared. The LLZO fibers play a great role in facilitating the transport of lithium ions,

make the CSE possessing high electrochemical window, ion transport number, and an ionic conductivity. While the viscoelastic PPO provides high mechanical and heat-resistance properties for the electrolyte. This design is helpful for the preparation of high-performance solid electrolyte in high-voltage lithium battery.

**Supplementary Information** The online version contains supplementary material available at <https://doi.org/10.1007/s00339-024-07815-x>.

**Acknowledgements** The work was financially supported by National Natural Science Foundation of China (No. 51474113), Technical Innovation Project of Yangzhou Junhe Film Technology Co., (No. HX20240466) and Science and Technology Plan Project of Xuancheng City (urban linkage 2023-5).

**Author contributions** Liang Zhong and Jie Li (Investigation, writing original-draft), Zhi-xiong Chen, Li-ping Zhou, and Hai-xia Liu (theory analysis for electrochemistry), Mao-xiang Jing (supervisor, experimental design).

**Data availability** The authors confirm that the data supporting the findings of this study are available within the article [and/or] its supplementary materials.

## Declarations

**Conflict of interest** The authors declare that they have no conflicts of interest to this work.

## References

- Z. Gao, H. Sun, L. Fu, F. Ye, Y. Zhang, W. Luo, Y. Huang, Promises, Challenges, and recent progress of Inorganic Solid-State Electrolytes for all-solid-state Lithium batteries. *Adv. Mater.* **30**(17), 1705702 (2018). <https://doi.org/10.1002/adma.201705702>
- H. Yang, M.-. Jing, H.-. Li, W.-. Yuan, B. Deng, Q.-. Liu, B.-. Ju, X.-. Zhang, S. Hussain, X.-. Shen, X. Yan, -h. ‘Environment-friendly’ polymer solid electrolyte membrane via a rapid surface-initiating polymeration strategy. *Chem. Eng. J.* **421**, 129710 (2021). <https://doi.org/10.1016/j.cej.2021.129710>
- C. Sun, J. Liu, Y. Gong, D.P. Wilkinson, J. Zhang, Recent advances in all-solid-state rechargeable lithium batteries. *Nano Energy.* **33**, 363–386 (2017). <https://doi.org/10.1016/j.nanoen.2017.01.028>
- W. Zhang, J. Nie, F. Li, Z.L. Wang, C. Sun, A durable and safe solid-state lithium battery with a hybrid electrolyte membrane. *Nano Energy.* **45**, 413–419 (2018). <https://doi.org/10.1016/j.nanoen.2018.01.028>
- M.S. Shalaby, M.O. Alziyadi, H. Gamal, S. Hamdy, Solid-state lithium-ion battery: the key components enhance the performance and efficiency of anode, cathode, and solid electrolytes. *J. Alloys Compd.* **969**, 172318 (2023). <https://doi.org/10.1016/j.jallcom.2023.172318>
- T. Yang, C. Wang, W. Zhang, Y. Xia, H. Huang, Y. Gan, X. He, X. Xia, X. Tao, J. Zhang, A critical review on composite solid electrolytes for lithium batteries: design strategies and interface engineering. *J. Energy Chem.* **84**, 189–209 (2023). <https://doi.org/10.1016/j.jechem.2023.05.011>

7. J.A. Isaac, D. Devaux, R. Bouchet, Dense inorganic electrolyte particles as a lever to promote composite electrolyte conductivity. *Nat. Mater.* **21**(12), 1412–1418 (2022). <https://doi.org/10.1038/s41563-022-01343-w>
8. J. Zheng, Y.-Y. Hu, New insights into the compositional dependence of Li-Ion Transport in Polymer–Ceramic Composite Electrolytes. *ACS Appl. Mater. Interfaces.* **10**(4), 4113–4120 (2018). <https://doi.org/10.1021/acsami.7b17301>
9. H.-. Xu, M.-. Jing, Z.-. Huang, J. Li, T.-. Wang, W.-. Yuan, B.-. Ju, X. Shen, -q. cross-linked polypropylene oxide solid Electrolyte Film with enhanced mechanical, thermal, and Electrochemical properties via Additive Modification. *ACS Appl. Polym. Mater.* **3**(12), 6539–6547 (2021). <https://doi.org/10.1021/acsapm.1c01248>
10. Z.-. Huang, J. Li, L.-. Li, H.-. Xu, C. Han, M.-. Liu, J. Xiang, X.-. Shen, M. Jing, -x. boosting lithium-ion transport capability of LAGP/PPO composite solid electrolyte via component regulation from ‘Ceramics-in-polymer’ to ‘Polymer-in-ceramics’. *Ceram. Int.* **48**(18), 25949–25957 (2022). <https://doi.org/10.1016/j.ceramint.2022.05.274>
11. N. Lv, Q. Zhang, Y. Xu, H. Li, Z. Wei, Z. Tao, Y. Wang, H. Tang, PEO-based composite solid electrolyte for lithium battery with enhanced interface structure. *J. Alloys Compd.* **938**, 168675 (2023). <https://doi.org/10.1016/j.jallcom.2022.168675>
12. M.-. Jing, H. Yang, H. Chong, F. Chen, L.-. Zhang, X.-. Hu, F.-. Tu, X. Shen, -q. Synergistic Enhancement effects of LLZO fibers and interfacial modification for polymer solid electrolyte on the ambient-temperature Electrochemical performances of solid-state battery. *J. Electrochem. Soc.* **166**(13), A3019–A3027 (2019). <https://doi.org/10.1149/2.1171913jes>
13. X. Zhang, T. Liu, S. Zhang, X. Huang, B. Xu, Y. Lin, B. Xu, L. Li, C.-W. Nan, Y. Shen, Synergistic coupling between Li<sub>6</sub>.75La<sub>3</sub>Zr<sub>1</sub>.75Ta<sub>0</sub>.25O<sub>12</sub> and poly (vinylidene fluoride) induces high ionic conductivity, mechanical strength, and thermal stability of solid composite electrolytes. *J. Am. Chem. Soc.* **139**(39), 13779–13785 (2017). <https://doi.org/10.1021/jacs.7b06364>
14. X.-. Hu, M.-. Jing, H. Yang, Q.-. Liu, F. Chen, W.-. Yuan, L. Kang, D.-. Li, X. Shen, -q. enhanced ionic conductivity and lithium dendrite suppression of polymer solid electrolytes by alumina nanorods and interfacial graphite modification. *J. Colloid Interface Sci.* **590**, 50–59 (2021). <https://doi.org/10.1016/j.jcis.2021.01.018>
15. L. Zhu, P. Zhu, S. Yao, X. Shen, F. Tu, High-performance solid PEO/PPC/LLTO-nanowires polymer composite electrolyte for solid-state lithium battery. *Int. J. Energy Res.* **43**(9), 4854–4866 (2019). <https://doi.org/10.1002/er.4638>
16. W. Liu, N. Liu, J. Sun, P.-C. Hsu, Y. Li, H.-W. Lee, Y. Cui, Ionic conductivity enhancement of polymer electrolytes with ceramic nanowire fillers. *Nano Lett.* **15**(4), 2740–2745 (2015). <https://doi.org/10.1021/acs.nanolett.5b00600>
17. M.B. Mohamed, M.H. Abdel-Kader, A.A. Alhazime, Structural and optical properties of doped ZnO/SiO<sub>2</sub> nanocomposite. *Int. J. Appl. Ceram. Technol.* **16**(3), 1209–1217 (2019). <https://doi.org/10.1111/ijac.13156>
18. M.B. Mohamed, M. Abdel-Kader, Effect of excess oxygen content within different nano-oxide additives on the structural and optical properties of PVA/PEG blend. *Appl. Phys. A* **125**, 1–11 (2019). <https://doi.org/10.1007/s00339-019-2492-1>
19. M.B. Mohamed, M. Abdel-Kader, SnS<sub>2</sub>/polycarbonate nanocomposites: structural and optical characterizations. *J. Inorg. Organomet. Polym. Mater.* **30**(6), 2289–2298 (2020). <https://doi.org/10.1007/s10904-019-01364-0>
20. J. Li, L. Zhu, J. Xu, M. Jing, S. Yao, X. Shen, S. Li, F. Tu, Boosting the performance of poly(ethylene oxide)-based solid polymer electrolytes by blending with poly(vinylidene fluoride-co-hexafluoropropylene) for solid-state lithium-ion batteries. *Int. J. Energy Res.* **44**(9), 7831–7840 (2020). <https://doi.org/10.1002/er.5476>
21. P.-A. Le, N.T. Nguyen, P.L. Nguyen, T.V.B. Phung, C.D. Do, A mini review of current studies on metal-organic frameworks-incorporated composite solid polymer electrolytes in all-solid-state lithium batteries. *Heliyon.* **9**(9), e19746 (2023). <https://doi.org/10.1016/j.heliyon.2023.e19746>
22. L.-. Zhang, H.-. Xu, M.-. Jing, L.-. Li, H. Yang, X. Shen, -q. solid Electrolyte/Lithium Anodes stabilized by reduced Graphene Oxide interlayers: implications for solid-state Lithium batteries. *ACS Appl. Nano Mater.* **4**(9), 9471–9478 (2021). <https://doi.org/10.1021/acsanm.1c01932>
23. F. Chen, M.-. Jing, H. Yang, W.-. Yuan, M.-. Liu, Y.-. Ji, S. Hussain, X. Shen, -q. improved ionic conductivity and Li dendrite suppression of PVDF-based solid electrolyte membrane by LLZO incorporation and mechanical reinforcement. *Ionics.* **27**(3), 1101–1111 (2021). <https://doi.org/10.1007/s11581-020-03891-0>
24. M. Wu, D. Liu, D. Qu, Z. Xie, J. Li, J. Lei, H. Tang, 3D coral-like LLZO/PVDF composite electrolytes with enhanced ionic conductivity and mechanical flexibility for solid-state Lithium batteries. *ACS Appl. Mater. Interfaces.* **12**(47), 52652–52659 (2020). <https://doi.org/10.1021/acsami.0c15004>
25. J. Li, R. Li, L.-. Li, H. Yang, M.-. Liu, J. Xiang, S. Hussain, X.-. Shen, M. Jing, -x. A high-filled Li<sub>7</sub>La<sub>3</sub>Zr<sub>2</sub>O<sub>12</sub>/Polypropylene Oxide Composite Solid Electrolyte with Improved Lithium-Ion Transport and Safety performances for High-Voltage Li batteries. *ACS Appl. Energy Mater.* **5**(9), 10786–10793 (2022). <https://doi.org/10.1021/acsaeam.2c01487>
26. T. Yang, J. Zheng, Q. Cheng, Y.-Y. Hu, C.K. Chan, Composite Polymer Electrolytes with Li<sub>7</sub>La<sub>3</sub>Zr<sub>2</sub>O<sub>12</sub> Garnet-Type nanowires as ceramic fillers: mechanism of Conductivity Enhancement and Role of Doping and morphology. *ACS Appl. Mater. Interfaces.* **9**(26), 21773–21780 (2017). <https://doi.org/10.1021/acsami.7b03806>
27. J. Li, M.-. Jing, R. Li, L.-. Li, Z.-. Huang, H. Yang, M.-. Liu, S. Hussain, J. Xiang, Shen, X.-q. Al<sub>2</sub>O<sub>3</sub> Fiber-Reinforced Polymer Solid Electrolyte films with Excellent Lithium-Ion Transport Properties for high-voltage solid-state Lithium batteries. *ACS Appl. Polym. Mater.* **4**(10), 7144–7151 (2022). <https://doi.org/10.1021/acsapm.2c01034>
28. J. Sharma, G. Polizos, C.J. Jafta, D.L. Wood, J. Li, Review—Electrospun Inorganic Solid-State Electrolyte fibers for Battery Applications. *J. Electrochem. Soc.* **169**(5), 050527 (2022). <https://doi.org/10.1149/1945-7111/ac6c1c>
29. S. Saran, Y.R. Eker, Synthesis, structural and conductive properties of Nd doped garnet-type Li<sub>7</sub>La<sub>3</sub>Zr<sub>2</sub>O<sub>12</sub> Li-ion conductor. *Current Applied Physics* **2022**, *41*, 1–6. <https://doi.org/10.1016/j.cap.2022.06.004>
30. Z. Zhang, Y. Huang, H. Gao, J. Huang, C. Li, P. Liu, An all-solid-state lithium battery using the Li<sub>7</sub>La<sub>3</sub>Zr<sub>2</sub>O<sub>12</sub> and Li<sub>6</sub>.7La<sub>3</sub>Zr<sub>1</sub>.7Ta<sub>0</sub>.3O<sub>12</sub> ceramic enhanced polyethylene oxide electrolytes with superior electrochemical performance. *Ceram. Int.* **46**(8), 11397–11405 (2020). <https://doi.org/10.1016/j.ceramint.2020.01.170>
31. T.H. Mengesha, S.L. Beshahwured, S.-H. Wu, Y.-S. Wu, R. Jose, S.J. Lue, C.-C. Yang, Freestanding Trilayer Hybrid Solid Electrolyte with Electrospun Interconnected Al-LLZO nanofibers for solid-state Lithium-metal batteries. *ACS Appl. Energy Mater.* **4**(12), 14554–14574 (2021). <https://doi.org/10.1021/acsaeam.1c03202>
32. H.-. Xu, M.-. Jing, J. Li, Z.-. Huang, T.-. Wang, W.-. Yuan, B.-. Ju, X. Shen, -q. safety-enhanced flexible polypropylene Oxide–ZrO<sub>2</sub> Composite Solid Electrolyte Film with High Room-Temperature Ionic Conductivity. *ACS Sustain. Chem. Eng.* **9**(33), 11118–11126 (2021). <https://doi.org/10.1021/acssuschemeng.1c02886>



33. H. Chen, Q.-. Liu, M.-. Jing, F. Chen, W.-. Yuan, B.-. Ju, F.-. Tu, X.-. Shen, S. Qin, -b. Improved Interface Stability and Room-Temperature performance of solid-state Lithium batteries by Integrating Cathode/Electrolyte and Graphite Coating. *ACS Appl. Mater. Interfaces*. **12**(13), 15120–15127 (2020). <https://doi.org/10.1021/acsami.9b22690>
34. J. Li, L. Zhong, J.-. Li, H.-. Wu, W.-. Shao, P.-. Wang, M.-. Liu, G. Zhang, M. Jing, -x. insights into the effects of different inorganic fillers on the electrochemical performances of polymer solid electrolytes. *Colloids Surf., a* **671**, 131704 (2023). <https://doi.org/10.1016/j.colsurfa.2023.131704>
35. Y. Zhao, J. Yan, W. Cai, Y. Lai, J. Song, J. Yu, B. Ding, Elastic and well-aligned ceramic LLZO nanofiber based electrolytes for solid-state lithium batteries. *Energy Storage Mater.* **23**, 306–313 (2019). <https://doi.org/10.1016/j.ensm.2019.04.043>
36. Z. Wen, Y. Li, Z. Zhao, W. Qu, N. Chen, Y. Xing, Y. Ma, L. Li, F. Wu, R. Chen, A leaf-like Al<sub>2</sub>O<sub>3</sub>-based quasi-solid electrolyte with a fast Li<sup>+</sup>-conductive interface for stable lithium metal anodes. *J. Mater. Chem. A* **8**(15), 7280–7287 (2020). <https://doi.org/10.1039/d0ta02098b>
37. Z. Ren, J. Li, Y. Gong, C. Shi, J. Liang, Y. Li, C. He, Q. Zhang, X. Ren, Insight into the integration way of ceramic solid-state electrolyte fillers in the composite electrolyte for high performance solid-state lithium metal battery. *Energy Storage Mater.* **51**, 130–138 (2022). <https://doi.org/10.1016/j.ensm.2022.06.037>
38. R. Li, J. Li, L.-. Li, H. Yang, G. Zhang, J. Xiang, X.-. Shen, M. Jing, -x. A bifunctional composite artificial solid electrolyte interphase for high stable solid-state lithium batteries. *Colloids Surf., a* **657**, 130600 (2023). <https://doi.org/10.1016/j.colsurfa.2022.130600>
39. K.H. Kim, J.H. Cho, J.U. Hwang, J.S. Im, Y.-S. Lee, A key strategy to form a LiF-based SEI layer for a lithium-ion battery anode with enhanced cycling stability by introducing a semi-ionic C F bond. *J. Ind. Eng. Chem.* **99**, 48–54 (2021). <https://doi.org/10.1016/j.jiec.2021.04.002>
40. S.L. Beshahwured, Y.-S. Wu, T.B. Truong, R. Jose, C.-C. Yang, A modified trilayer membrane for suppressing Li dendrite growth in all-solid-state lithium-metal batteries. *Chem. Eng. J.* **426**, 131850 (2021). <https://doi.org/10.1016/j.ccej.2021.131850>

**Publisher's Note** Springer Nature remains neutral with regard to jurisdictional claims in published maps and institutional affiliations.

Springer Nature or its licensor (e.g. a society or other partner) holds exclusive rights to this article under a publishing agreement with the author(s) or other rightsholder(s); author self-archiving of the accepted manuscript version of this article is solely governed by the terms of such publishing agreement and applicable law.